Journal of Organometallic Chemistry 882 (2019) 80–89

Contents lists available at ScienceDirect

Journal of Organometallic Chemistry

journal homepage: www.elsevier.com/locate/jorganchem

Preparation and self-assembly of polyferrocenyldimethylsilane-containing tri- and pentablock terpolymers

Christian Rüttiger [a], Lea Gemmer [a], Sebastian Schöttner [a], Björn Kuttich [b], Bernd Stühn [b], Markus Gallei [a, *]

[a] Ernst-Berl-Institute of Chemical Engineering and Macromolecular Science, Technische Universität Darmstadt, Alarich-Weiss-Str. 4, D-64287, Darmstadt, Germany
[b] Institute of Condensed Matter Physics, Technische Universität Darmstadt, Hochschulstraße 8, D-64289, Darmstadt, Germany

ARTICLE INFO

Article history:
Received 29 October 2018
Received in revised form
19 December 2018
Accepted 3 January 2019
Available online 4 January 2019

Keywords:
Metallopolymers
Block copolymers
Morphology
Anionic polymerization
Ferrocenes

ABSTRACT

Functional block copolymers (BCPs) featuring metal moieties are a unique class of materials because of their switching capabilities and pronounced microphase separation behaviour. Within this work, ABC and CBABC tri- and pentablock terpolymers consisting of polystyrene (PS), poly(1,1′-dimethylsilaferrocenophane) (PFS) and a third block segment C either consisting of poly(methyl methacrylate) (PMMA) or poly(2-vinylpyridine) (P2VP) were synthesized via sequential living anionic polymerization. Well-defined polymers having molar masses up to 90 kg mol^{-1} and low dispersity index values, $Đ$, below 1.10 were obtained. The multi-functional BCPs were characterized with respect to their constitution and composition by size-exclusion chromatography (SEC) measurements and NMR spectroscopy. Focus of this work was to study the microphase separation of the metal-containing tri- and pentablock terpolymers by (scanning) transmission electron microscopy (TEM) and small-angle X-ray scattering (SAXS) measurements. Highly ordered structures at the nanoscale were observed comprising lamellar or cylindrical morphologies with more complex core-shell cylindrical morphologies for the organometallic block segment. This structure formation was more pronounced in case of P2VP-containing ABC terblock copolymers. Finally, synthetic approaches for the preparation of CBABC pentablock terpolymers were presented and the obtained bulk morphologies of these polymers were investigated by TEM and SAXS measurements.

© 2019 Elsevier B.V. All rights reserved.

1. Introduction

Block copolymers (BCP) have garnered significant attention because of their capability of forming fascinating nanostructures comprising lamellae, cylinders, spheres or more complex (co) continuous morphologies [1–3]. As a consequence, BCPs have found applications in many diverse areas including nanolithography, drug delivery, and separation technologies [4–9]. Moreover, so-called *smart* or functional BCPs featuring chemically or physically addressable building blocks can be designed to alter polymer conformation, solubility, or even covalent linkages, as a function of external triggers. Common stimuli include temperature, pH, light, redox reagents and electrical fields [10–18]. For instance, BCPs featuring polyvinylpyridine (PVP) block segments and their microphase-separated structures are capable of complexing metal ions or nanoparticles within their segregated domains [19].

Functional BCPs featuring metal centers – like the ferrocene moiety – and which consist of two or more block segments are much less investigated regarding their nano structure formation, especially in the bulk state. In general, such metal-containing polymers – also referred to as *metallopolymers* – are potential candidates for many different applications and readers are referred to comprehensive reviews, as given by Zhou et al. [13], the Tang group [20–22], and other authors [23–25]. Enormous efforts of the scientific community in terms of the design of complex and functional BCPs have been carried out during the last decade, but there are still significant challenges to overcome. In the field of metallopolymers, a synthetic breakthrough for the preparation of switchable ferrocene-containing polymers having the metal centers as part of the polymer main chain, was the ring-opening polymerization (ROP) of strained *ansa*-metallocenophanes. The most prominent example is the 1,1′-dimethylsilaferrocenophane (FS) monomer, found by Manners and co-workers [26–29]. Since Manners' discovery, high-molecular weight polyferrocenylsilanes

* Corresponding author.
E-mail address: m.gallei@mc.tu-darmstadt.de (M. Gallei).

https://doi.org/10.1016/j.jorganchem.2019.01.001
0022-328X/© 2019 Elsevier B.V. All rights reserved.

(PFS) and a manifold of PFS-based diblock copolymers with interesting properties were synthesized [13].

In general, the design and addition of a third polymer block segment leads to the formation of ABC triblock terpolymers. Compared to the above-mentioned diblock copolymers, an increase up to more than 30 possible and complex morphologies can be observed by varying the kind of polymers and their block lengths [30–33]. Additionally, the order of the block segments A, B and C and their corresponding Flory-Huggins interaction parameters χ (χ_{AB}, χ_{BC}, χ_{AC}) are some reasons for the large number of different morphologies, while the size of the BCP domains is controlled by the degree of polymerization, *N* [30,34]. From a polymer chemist's point of view, the most thoroughly investigated morphologies for ABC triblock terpolymers in the bulk state are polystyrene-*block*-polybutadiene-*block*-poly(methyl methacrylate) (SBM) and polystyrene-*block*-poly(ethylene-*co*-butylene)-*block*-poly(methyl methacrylate) (SEBM), as investigated by Krausch, Abetz and Stadler [35,36], or polystyrene-*block*-polybutadiene-*block*-poly(vinylpyridine)s (SBV) [37].

In general, controlled or living polymerization methods are widely used for the preparation of such polymer architectures, both including ABC and symmetric CBABC pentablock terpolymers. The latter multiblock terpolymers are less investigated, but some studies proved an improved mechanical stability making them also useful for practical applications like drug delivery or carrier systems [32,38–41]. In the field of metallopolymers, some studies on triblock terpolymers have been carried out, with much less for pentablock terpolymers. A recent study compares blends of functional diblock copolymers with polyvinylferrocene as metallopolymer with the corresponding triblock terpolymers for the preparation of nanocapsules [42]. As an important finding, the usability of the metal-containing triblock terpolymers turned out to be advantageous with respect to microphase separation and triggered release properties compared to the corresponding blend systems. PFS-containing triblock terpolymers [43] and their interesting and complex morphologies have been reported for PS-*b*-PI-*b*-PFS for the preparation of square-symmetry microdomains [44] and as magnetic templates [45], star polymers for PS, PI and PFS with alternating cylinders and two different Archimedean tiling patterns [46], for PS-*b*-PFS-*b*-PMMA [47] and a first communication on PS-*b*-PFS-*b*-P2VP [48]. In the field of symmetric pentablock terpolymers having two PFS segments (PMMA-*b*-PFS-*b*-PS-*b*-PFS-*b*-PMMA), Datta and Rehahn reported first results on the bulk morphology within a communication [49].

Within the present work, the preparation of P2VP-*b*-PFS-*b*-PS-*b*-PFS-*b*-P2VP and PMMA-*b*-PFS-*b*-PS-*b*-PFS-*b*-PMMA pentablock terpolymers as well as the corresponding linear triblock terpolymers have been synthesized by using living anionic polymerization strategies. The tri- and pentablock terpolymers have been studied with respect to their composition and thermal properties by ^{1}H NMR spectroscopy, size exclusion chromatography (SEC), and differential scanning calorimetry (DSC). A focus of this work was to gain insights into the microphase separation by transmission electron microscopy (TEM) and small-angle X-ray scattering (SAXS) measurements. For all designed terpolymers, microphase separation occurred leading to interesting morphologies at the nanometer length scale.

2. Experimental section

2.1. Reagents

All solvents and reagents were purchased from Alfa Aesar (Haverhill, MA, USA), Sigma-Aldrich (St. Louis, MA, USA), Fisher Scientific (Hampton, NH, USA), ABCR (Karlsruhe, Germany) and used as received unless otherwise stated. Deuterated solvents were purchased from Sigma-Aldrich. Tetrahydrofuran (THF) was distilled from sodium/benzophenone prior to the addition of 1,1′-diphenylethylene (DPE) and *n*-butyllithium (*n*-BuLi) followed by a second cryo-transfer. Styrene (S), methyl methacrylate (MMA), 2-vinylpyridine (2VP) and 1,1′dimethylsilacyclobutane (DMSB) were dried by stirring over calcium hydride (CaH_2) or trioctylaluminium and cryo-transferred prior to use. 1,1′-dimethylsilaferrocenophane (FS) [50] was synthesized and purified described elsewhere. Lithium chloride (LiCl) was dissolved in a small amount of freshly distilled THF and treated with *sec*- butyllithium. After stirring at room temperature for 1 h, THF was removed *in vacuo* and dried LiCl was transferred and stored in a glovebox. DPE was dried by adding a small amount of *n*-BuLi followed by cryo-transfer. All syntheses were carried out under an atmosphere of nitrogen or argon using Schlenk techniques or a glovebox equipped with a coldwell apparatus.

2.2. Instrumentation

NMR spectra were recorded on a Bruker DRX 300 spectrometer (Billerica, MA, USA) working at 300 MHz. NMR chemical shifts are referenced relative to the used solvent. Standard size-exclusion chromatography (SEC) was performed with a system composed of a 1260 IsoPump – G1310B - (Agilent Technologies, Santa Clara, CA, USA), a 1260 VW-detector – G1314F – at 254 nm (Agilent Technologies) and a 1260 RI-detector – G1362A – at 30 °C (Agilent Technologies), THF as the mobile phase (flow rate 1 mL min^{-1}) on a SDV column set from PSS (Polymer Standard Service (PSS), Mainz, Germany) (SDV 10^3, SDV 10^5, SDV 10^6). Calibration was carried out using PS standards (from PSS). For data acquisition and evaluation of the measurements, PSS WinGPC® UniChrom 8.2 was used. For determining the thermal properties of the synthesized polymers, differential scanning calorimetry (DSC) was performed with a Mettler Toledo DSC-1 (Columbus, OH, USA) in a temperature range of −20 °C to 170 °C with a heating rate of 10 K min^{-1} under nitrogen atmosphere. Second heat run was used for evaluation of thermal properties by using Mettler Toledo STARe®14 software. Transmission electron microscopy (TEM) experiments were carried out using a Zeiss EM 10 electron microscope (Oberkochen, Germany) operating at 60 kV with a slow-scan CCD camera obtained from TRS (Tröndle, Morrenweis, Germany) in bright field mode or a JEOL JEM-2100F microscope (JEOL, Tokyo, Japan) equipped with a field emission gun operating at a nominal acceleration voltage of 200 kV. The 2100F was operated in scanning TEM (STEM) mode. The samples were investigated using a JEOL single tilt holder. Small angle X-ray scattering (SAXS) was performed using a laboratory set-up (Molecular Metrology, Northampton, MA, USA). We used the Kα-line of a copper X-ray tube with a wavelength of $\lambda = 1.54$ Å monochromated and focused by a X-ray mirror and collimated by a pinhole collimation system. Data were recorded on a 2-D multiwire detector. Since all samples scattered isotropically data was radially averaged resulting in intensity vs. magnitude of the scattering vector $q=(4\pi/\lambda)\sin\theta$, with 2θ denoting the scattering angle. With the given sample-detector distance of 1.5 m, the accessible range of scattering vectors was $0.008\ \text{Å}^{-1} \leq q \leq 0.25\ \text{Å}^{-1}$. q-scaling was calibrated by measuring silver behenate. The sample holder was sealed by aluminum foil.

2.3. Synthesis of linear triblock terpolymers

2.3.1. Synthesis of PS_{211}-*b*-PFS_{37}-*b*-$PMMA_{437}$

In an ampule equipped with a stirring bar, 600 mg (5.76 mmol) styrene was dissolved in 40 mL of dry THF and the solution was cooled down to −78 °C. The polymerization was initiated by quick

addition of 19.3 μL s-BuLi (0.025 mmol, 1.3 M solution in hexane) with a syringe. The solution was stirred for 1 h to ensure complete conversion. After taking an aliquot for SEC measurement, 200 mg (0.83 mmol) FS dissolved in 1 mL THF was quickly added with a syringe and the reaction was stirred for 3 h at room temperature. An aliquot was taken for SEC and NMR measurement and 18 μL (0.13 mmol) DPE and 6.4 μL (0.05 mmol) DMSB were added. After 1 h at room temperature, 5 mL THF with 10.5 mg LiCl (0.25 mmol, 10 Äq) were added. The reaction mixture was cooled down to −78 °C and 620 mg (6.19 mmol) MMA was quickly added. After 13 h the polymerization was terminated by the addition a small amount of degassed methanol and the polymer was poured into a 10-fold excess of methanol. The polymer was collected by filtration, washed several times with methanol, dried under vacuum (1.31 g). For separation of residual PS and PS-*b*-PFS polymer impurities, a part of the polymer mixture was again dissolved in THF followed by the dropwise addition of *n*-hexane until the polymer precipitated. The polymer fraction was collected by filtration and dried *in vacuo*.

SEC (vs PS): PS: $M_n = 22\,000$ g mol^{-1}; $M_w = 22\,700$ g mol^{-1}; $Đ = 1.03$.

PS-*b*-PFS: $M_n = 28\,500$ g mol^{-1}; $M_w = 29\,900$ g mol^{-1}; $Đ = 1.05$.

PS-*b*-PFS-*b*-PMMA: $M_n = 63\,300$ g mol^{-1}; $M_w = 64\,600$ g mol^{-1}; $Đ = 1.02$.

^{1}H-NMR (300 MHz, 300 K, $CDCl_3$, δ in ppm): 7.20–6.91 (m, 3-$H_{4/5}$), 6.81–6.36 (m, 2-H_3), 4.25 (s, 4-H_8), 4.04 (s, 4-H_7), 3.60 (s, 3-H_{11}), 2.03–0.80 (m, backbone $H_{1/2/9/10}$), 0,40 (s, 6-H_6).

2.3.2. Synthesis of PS_{250}-*b*-PFS_{39}-*b*-$P2VP_{551}$

In an ampule equipped with a stirring bar, 600 mg (5.76 mmol) styrene was dissolved in 40 mL of dry THF and the solution was cooled down to −78 °C. The polymerization was initiated by quick addition of 19.3 μL s-BuLi (0.025 mmol, 1.3 M solution in hexane) with a syringe. The solution was stirred for 1 h to ensure complete conversion. After taking an aliquot for SEC measurement, 200 mg (0.83 mmol) FS dissolved in 1 mL THF was quickly added with a syringe and the reaction was stirred for 3 h at room temperature. An aliquot was taken for SEC and NMR measurement and 18 μL (0.13 mmol) DPE and 6.4 μL (0.05 mmol) DMSB were added. After 1 h 5 mL THF with 10.5 mg LiCl (0.25 mmol, 10 Äq) were added. The reaction mixture was cooled down to −78 °C and 600 mg (5.71 mmol) 2VP was quickly added. After 13 h the polymerization was terminated by the addition a small amount of degassed methanol and the polymer was poured into a 10-fold excess of methanol. The polymer was collected by filtration, washed several times with methanol, dried under vacuum (1.29 g). For separation of residual PS and PS-*b*-PFS polymer impurities, a part of the polymer mixture was again dissolved in THF followed by the dropwise addition of water until the polymer precipitated. The polymer fraction was collected by filtration and dried *in vacuo*.

SEC (vs **PS):** PS: $M_n = 26\,000$ g mol^{-1}; $M_w = 28\,000$ g mol^{-1}; $Đ = 1.08$.

PS-*b*-PFS: $M_n = 31\,900$ g mol^{-1}; $M_w = 35\,100$ g mol^{-1}; $Đ = 1.10$.

PS-*b*-PFS-*b*-P2VP: $M_n = 72\,800$ g mol^{-1}; $M_w = 79\,400$ g mol^{-1}; $Đ = 1.09$.

^{1}H-NMR (300 MHz, 300 K, $CDCl_3$, δ in ppm): 8.40–8.08 (m, 1-H_{11}), 7.26–6.20 (m, 8-$H_{3\text{-}5/12\text{-}14}$), 4.21 (s, 4-$H_8$), 4.01 (s, 4-$H_7$) 2.30–1.26 (m, backbone $H_{1/2/9/10}$), 0.45 (m, 6-H_6).

2.4. Synthesis of symmetrical pentablock terpolymers

2.4.1. Synthesis of PS_{230}-(*b*-PFS_{15}-*b*-$PMMA_{118}$)$_2$

In an ampule equipped with a stirring bar, 660 mg (6.34 mmol) styrene was dissolved in 40 mL of dry THF and the solution was cooled down to −78 °C. The polymerization was initiated by quick addition of 61 μL lithium naphthalenide (0.055 mmol, 0.9 M solution in THF) with a syringe. The solution was stirred for 1 h to ensure complete conversion. After taking an aliquot for SEC measurement, 220 mg (0.91 mmol) FS dissolved in 1 mL THF was quickly added with a syringe and the reaction was stirred for 3 h at room temperature. An aliquot was taken for SEC and NMR measurement and 38.8 μL (0.27 mmol) DPE and 14.1 μL (0.11 mmol) DMSB were added. After 1 h 3 mL THF with 11 mg LiCl (0.26 mmol) were added. The reaction mixture was cooled down to −78 °C and 670 mg (6.69 mmol) MMA was quickly added. After 10 h the polymerization was terminated by the addition a small amount of degassed methanol and the polymer was poured into a 10-fold excess of methanol. The polymer was collected by filtration, washed several times with methanol, dried under vacuum. (1.30 g).

SEC (vs **PS):** PS: $M_n = 23\,900$ g mol^{-1}; $M_w = 24\,800$ g mol^{-1}; $Đ = 1.03$.

PFS-*b*-PS-*b*-PFS: $M_n = 30\,800$ g mol^{-1}; $M_w = 33\,300$ g mol^{-1}; $Đ = 1.08$.

PMMA-*b*-PFS-*b*-PS-*b*-PFS-*b*-PMMA: $M_n = 45\,200$ g mol^{-1}; $M_w = 49\,300$ g mol^{-1}; $Đ = 1.09$.

^{1}H-NMR (300 MHz, 300 K, $CDCl_3$, δ in ppm): 7.20–6.90 (m, 3-$H_{4/5}$), 6.80–6.35 (m, 2-H_3), 4.22 (s, 4-H_8), 4.01 (s, 4-H_7), 3.60 (s, 3-H_{11}), 2.10–0.79 (m, backbone $H_{1/2/9/10}$), 0.45 (s, 6-H_6).

2.4.2. Synthesis of PS_{231}-(*b*-PFS_{16}-*b*-$P2VP_{95}$)$_2$

In an ampule equipped with a stirring bar, 600 mg (5.76 mmol) styrene was dissolved in 40 mL of dry THF and the solution was cooled down to −78 °C. The polymerization was initiated by quick addition of 56 μL lithium naphthalenide (0.05 mmol, 0.9 M solution in THF) with a syringe. The solution was stirred for 1 h to ensure complete conversion. After taking an aliquot for SEC measurement, 200 mg (0.83 mmol) FS dissolved in 1 mL THF was quickly added with a syringe and the reaction was stirred for 3 h at room temperature. An aliquot was taken for SEC and NMR measurement and 35 μL (0.25 mmol) DPE and 12.9 μL (0.1 mmol) DMSB were added. After 1 h 3 mL THF with 22 mg LiCl (0.52 mmol, 10 Äq) were added. The reaction mixture was cooled down to −78 °C and 590 mg (5.61 mmol) 2VP was quickly added. After 13 h the polymerization was terminated by the addition a small amount of degassed methanol and the polymer was poured into a 10-fold excess of methanol. The polymer was collected by filtration, washed several times with methanol, dried under vacuum. (1.18 g).

SEC (vs PS): PS: $M_n = 24\,100$ g mol^{-1}; $M_w = 24\,800$ g mol^{-1}; $Đ = 1.03$.

PFS-*b*-PS-*b*-PFS: $M_n = 32\,600$ g mol^{-1}; $M_w = 36\,800$ g mol^{-1}; $Đ = 1.13$.

P2VP-*b*-PFS-*b*-PS-*b*-PFS-*b*-P2VP: $M_n = 43\,400$ g mol^{-1}; $M_w = 45\,400$ g mol^{-1}; $Đ = 1.05$.

^{1}H-NMR (300 MHz, 300 K, $CDCl_3$, δ in ppm): 8.289–8.06 (m, 1-H_{11}), 7.25–6.20 (m, 8-$H_{3\text{-}5/12\text{-}14}$), 4.21 (s, 4-$H_8$), 4.01 (s, 4-$H_7$) 2.35–1.26 (m, backbone $H_{1/2/9/10}$), 0.45 (m, 6-H_6).

3. Results and discussion

3.1. Synthesis of metallopolymer-containing tri- and pentablock terpolymers

Different triblock terpolymers and symmetrical pentablock terpolymers consisting of PS, PFS as metallopolymer and either PMMA or P2VP have been prepared according to Scheme 1 and Scheme 2. Starting from the polymerization of styrene **1**, which was initiated with *sec*-butyllithium as initiator in THF, 1,1′-dimethylsilaferrocenophane **3** has been added for the formation of PS-*b*-PFS macro-anions **4**. The final triblock terpolymers PS-*b*-PFS-*b*-PMMA **7** or PS-*b*-PFS-*b*-P2VP **9** were obtained after the addition of the corresponding monomers MMA or 2VP, respectively. The rather low

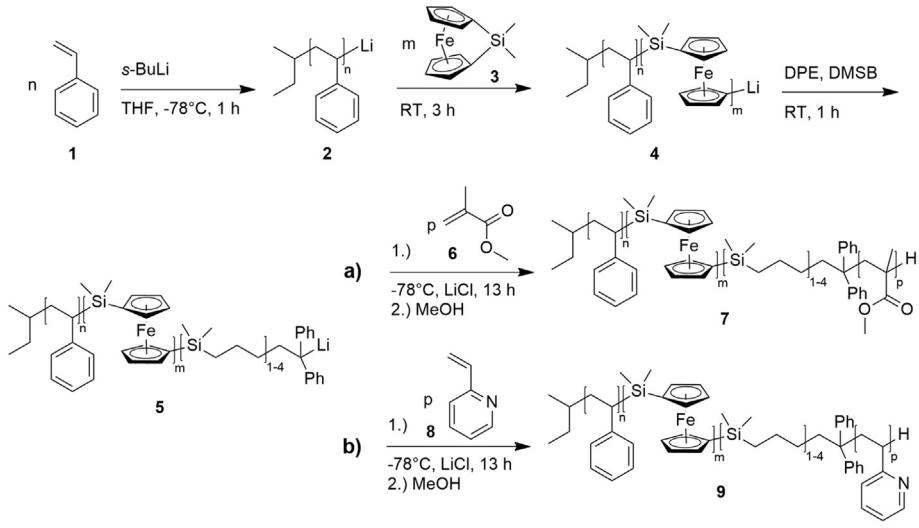

Scheme 1. Synthesis of triblock terpolymers PS-*b*-PFS-*b*-PMMA **7** and PS-*b*-PFS-*b*-P2VP **9** by sequential anionic polymerization of styrene **1**, initiated by *sec*-butyllithium at low temperatures followed by polymerization of 1,1′-dimethylsilaferrocenophane (FS) **3** at room temperature. After endfunctionalization with 1,1′-diphenylethylene (DPE) and 1,1′-dimethylsilacyclobutane (DMSB) **5** a) methyl methacrylate (MMA) **6** or b) 2-vinylpyridine (2VP) **8** was polymerized in the presence of LiCl at low temperatures.

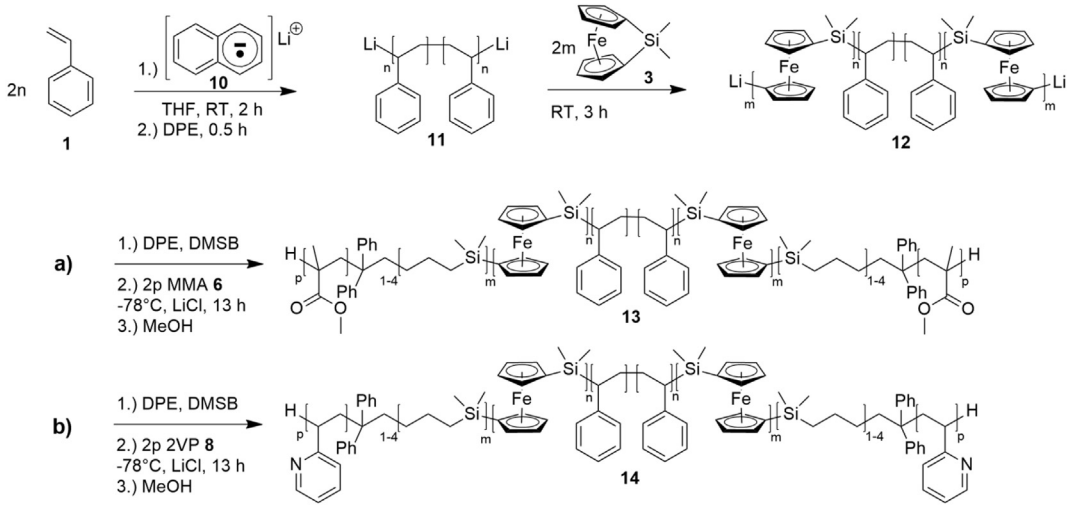

Scheme 2. Anionic polymerization of symmetric PS-(*b*-PFS-*b*-PMMA)$_2$ (**13**, a) or PS-(*b*-PFS-*b*-P2VP)$_2$ (**14**, b) pentablock terpolymer by initiation of styrene (**1**) with lithium naphthalenide (**10**) to obtain the bifunctional macroinitiator (**11**). After polymerization of FS monomer (**3**) and endcapping with DPE and DMSB at room temperature, a) MMA or b) 2VP is polymerized in the presence of LiCl at low temperatures.

reactivity of the FS living carbanion **4** can be overcome by increasing the temperature [51] or by the addition of the so-called carbanion pump, 1,1′dimethylsilacyclobutane (DMSB) [52] in order to increase the macro-anion chain end reactivity. Therefore, prior to the addition of MMA **6** or 2VP **8**, end-functionalization with 1,1′-diphenylethylene (DPE) and DMSB was carried out. The final triblock terpolymers are purified by inverse precipitation in order to remove small amounts of residual PS homopolymer and PS-*b*-PFS diblock copolymer impurities (see also experimental section).

In a similar way, the corresponding symmetric pentablock terpolymers PS-(*b*-PFS-*b*-PMMA)$_2$ **13** and PS-(*b*-PFS-*b*-P2VP)$_2$ **14** were prepared by sequential living anionic polymerization (Scheme 2), but with lithium naphthalenide **10** as bifunctional initiator for the anionic polymerization of styrene in order to prepare the bifunctional PS macro anion **11**.

All synthesized polymers were characterized by means of size-exclusion chromatography (SEC) and ^{1}H NMR spectroscopy to prove the successful polymerizations. The molar masses as well as dispersity index values, $Đ$, of PS, PS-*b*-PFS block segments and for the PS-(*b*-PFS-*b*-PMMA)$_2$ or PS-(*b*-PFS-*b*-P2VP)$_2$ were determined by SEC measurements vs. PS calibration in THF (exemplary Fig. 1 and also Figs. S1, S3, S5). Due to the fact that SEC measurements are based on the hydrodynamic radii of the polymers by using PS as standard, deviations for the metallopolymers can appear [53–55]. Therefore, the molar masses were additionally calculated by the molar ratio as determined by ^{1}H NMR spectroscopy (exemplary Fig. 2 and also Figs. S2, S4, S6) in combination with the molar mass of the PS homopolymers determined via SEC measurements vs. PS standards. Measured and calculated molar masses, M_n, dispersity index values, $Đ$, molar amounts, n_x, and volume contents, Φ_x, of PS, PFS and PMMA or P2VP are compiled in Table 1.

As can be concluded from Table 1, dispersity index values, $Đ$, of all polymers were in the range of 1.02–1.11 showing excellent control over the sequential anionic polymerization. Furthermore, for each tri- or pentablock terpolymer a significant increase of the measured or calculated molar mass could be obtained proving the

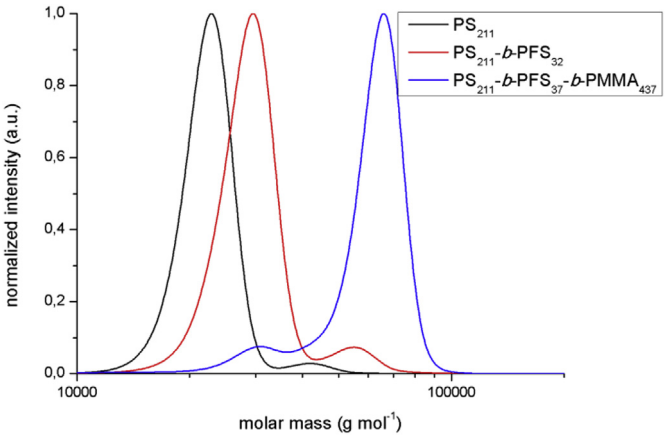

Fig. 1. Molar mass distributions obtained by SEC measurements vs. PS standards in THF as eluent for PS_{211} (black line), PS_{211}-*b*-PFS_{32} (red line) and PS_{211}-*b*-PFS_{37}-*b*-$PMMA_{437}$ (blue line). (For interpretation of the references to colour in this figure legend, the reader is referred to the Web version of this article.)

successful polymer chain extension after monomer addition. Comparisons of the overall molar masses determined by SEC measurements vs. PS standards and molar masses calculated by ^{1}H NMR data lead to a discrepancy of the obtained values. As mentioned before, this was due to the fact that SEC is a relative method and especially the hydrodynamic radii of synthesized tri- and pentablock terpolymers differ compared to SEC vs. PS standards. As a consequence the determined values derived from ^{1}H NMR data were closer to the absolute molar masses. These values were used in this study for subsequent calculations and interpretations on the obtained morphologies (*cf.* the following sections). Molar masses of the synthesized triblock terpolymers were 74.7 kg mol^{-1} for the PMMA – or 93.3 kg mol^{-1} for the P2VP-containing polymers. The corresponding triblock terpolymers were purified by inverse precipitation in order to reduce the amount of formed diblock copolymer impurities. In detail, by this step the amount of diblock copolymer of 38% after the sequential polymerization was reduced to 13%. The residual diblock copolymer precursors for both triblock terpolymer syntheses (SEC traces in Fig. 1 and Fig. S1, blue lines) were formed during the addition of DPE, DMSB and MMA or 2VP monomer, respectively. Volume fractions of 80% for PS and 20% for PFS were calculated for the final blend system based on ^{1}H NMR data for each diblock copolymer. The volume fractions for the purified triblock terpolymers differed slightly between, *i.e.* 32/11/57 for PS/PFS/PMMA and 29/9/62 for PS/PFS/P2VP. In the case of both pentablock terpolymers molar masses of 54.3 kg mol^{-1} and 51.8 kg mol^{-1} for the PMMA- and P2VP-containing polymer were obtained. Besides some impurities of about 14% of diblock copolymer precursor PS_{230}-(b-PFS_{15})$_2$, a slightly bimodal distribution was obtained within the molar mass distribution of the corresponding pentablock terpolymer PS_{230}-(b-PFS_{15}-b-$PMMA_{118}$)$_2$ (Fig. S3). This might be due to termination reactions during the polymerization of the third block segment. A possible explanation for the additional appearance of molar mass distribution compared to the P2VP-containing multiblock copolymers is the more reactive MMA repeating unit, allowing for backbiting and intermolecular reactions during anionic polymerization. SEC measurement of PS_{231}-(b-PFS_{16}-b-$P2VP_{95}$)$_2$ revealed an unimodal distribution and no significant residuals of PS_{230}-(b-PFS_{16})$_2$ precursor. Also, the calculated volume contents for both CBABC polymers revealed ratios of around 50% PS, 12% or 13% PFS and around 40% PMMA or P2VP, respectively (see Table 1). Thermal analysis was carried out using differential scanning calorimetry (DSC) measurements to further prove the preparation of tri- and pentablock terpolymers. Moreover, the presence of individual glass

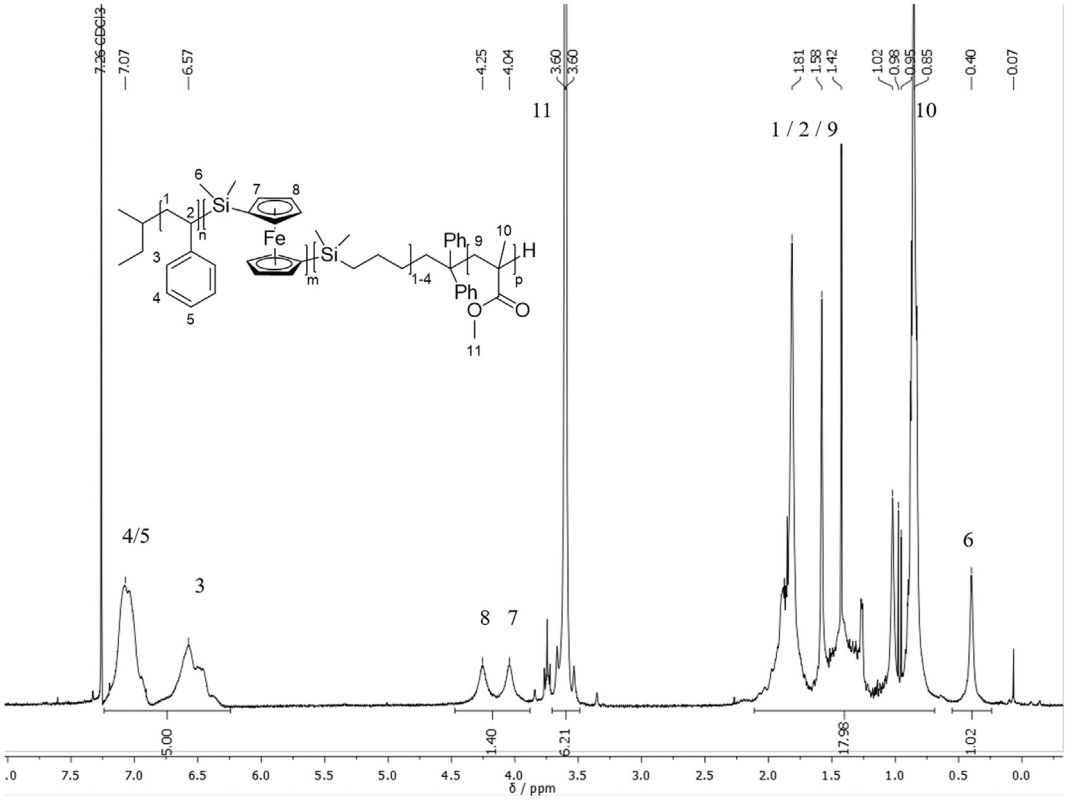

Fig. 2. ^{1}H NMR spectrum of PS_{211}-*b*-PFS_{37}-*b*-$PMMA_{437}$ in $CDCl_3$.

Table 1
Summarized molar masses (M_n) determined by SEC and ^{1}H NMR spectroscopy, dispersity index values ($Đ$), molar amount (n) and volume fraction (Φ) of PS, PFS and PMMA or P2VP of synthesized polymers calculated by SEC measurements and ^{1}H NMR spectroscopy.

Polymer	M_n [a]	M_n [b]	$Đ$ [c]	$n_{PS/PFS/PX}$ [d]	$\Phi_{PS/PFS/PX}$ [e]
PS_{211}	22.0	–	1.03		
PS_{211}-*b*-PFS_{32}	28.5	28.4	1.05	88/12	80/20
PS_{211}-*b*-PFS_{37}-*b*-$PMMA_{437}$	63.3	74.7	1.02	31/5/64	32/11/57
PS_{250}	26.0	–	1.08		
PS_{250}-*b*-PFS_{32}	31.9	33.7	1.10	88/12	80/20
PS_{250}-*b*-PFS_{39}-*b*-$P2VP_{551}$	72.8	93.3	1.09	30/5/65	29/9/62
PS_{230}	24.0	–	1.04		
PS_{230}-(*b*-PFS_{15})$_2$	30.8	30.9	1.07	88/12	80/20
PS_{230}-(*b*-PFS_{15}-*b*-$PMMA_{118}$)$_2$	45.2	54.3	1.09	47/6/47	47/12/41
PS_{231}	24.1	–	1.03		
PS_{231}-(*b*-PFS_{16})$_2$	32.6	31.4	1.11	88/12	80/20
PS_{231}-(*b*-PFS_{16}-*b*-$P2VP_{95}$)$_2$	43.4	51.8	1.05	51/7/42	49/13/38

[a] Molar masses in kg mol^{-1} determined by SEC (vs. PS standards, THF).
[b] Molar masses in kg mol^{-1} determined by ^{1}H NMR spectroscopy of block-, tri- and pentablock co- and terpolymers.
[c] $Đ$ values determined by SEC in THF.
[d] Molar amount (n_x) in % of PS, PFS, PMMA and P2VP calculated by ^{1}H NMR spectroscopy.
[e] Volume fraction (Φ) in % of PS, PFS, PMMA and P2VP estimated by using the densities of the corresponding homopolymers 1.05 g cm^{-3}, 1.26 g cm^{-3}, 1.18 g cm^{-3} and 1.15 g cm^{-3} [56,57], respectively.

transition temperatures, T_g, gives first evidences for microphase separation of the block segments. Measurements were performed for bulk samples of all tri- and pentablock terpolymers between −20 °C and 170 °C with a heat rate 10 K min^{-1} and all results are compiled in Table 2. The corresponding thermograms can be found in Fig. S7.

For all investigated polymers, glass transition temperatures, T_g, of around 100 °C could be observed, which correspond to PS or P2VP, respectively. However, a distinction between the T_g values of PS or P2VP cannot be observed because both T_g values are too close to each other. A characteristic T_g at about 128 °C could be found for syndiotactic PMMA [58]. While the T_g for PFS at around 30 °C is less pronounced, endothermic melting points, T_m, at around 130 °C were obtained for all polymers [59]. However, the T_m overlapped with the T_g for the PMMA segment. The less pronounced glass transition temperature for the PFS segment might be due to the low amount of PFS compared to PS, PMMA and P2VP and due to the presence of comparably short PFS chains.

In summary, the successful syntheses for the different tri- and pentablock terpolymers based on PS, PFS and PMMA or P2VP by means of sequential anionic polymerization were proven by SEC and ^{1}H NMR spectroscopy. Within the next section microphase separation of these multi-functional block terpolymers will be investigated by TEM and SAXS measurements.

3.2. Microphase separation of tri- and pentablock terpolymers

As described in the introduction, an increase with respect to structural complexity for ABC and CBABC terpolymers compared to AB block copolymers is expected. A large number of different self-assembled domains, which strongly depend on the polymer architecture, sequence and composition, are accessible. In order to investigate the microphase separation for all prepared tri- and pentablock terpolymers within this study, polymer bulk samples were prepared by dissolving the polymer in methylene chloride followed by slow evaporation of the solvent. In the next step, polymer samples were subjected to thermal annealing in an atmosphere of nitrogen at 160 °C for 36 h (triblock terpolymers) or 40 h (pentablock terpolymers), respectively. Ultrathin slices were prepared by ultramicrotoming and collected on TEM copper grids for TEM investigations. In the first part of this section, both synthesized ABC triblock terpolymers will be discussed in terms of self-assembly behavior examined by TEM and SAXS measurements. In Fig. 3, TEM images of polymer PS_{211}-*b*-PFS_{37}-*b*-$PMMA_{437}$ are given revealing a complex morphology with both lamellar and cylindrical separated domains. Considering the volume fraction of each block segment, PMMA with 57% represents the major component, which belongs to the bright lamellar domains. The lamellae distance between two bright lamellae was determined to be 37 ± 8 nm. On the other side, the PS segment (Φ_{PS} = 32%) formed the cylinders or together with the PFS segment the second lamellae. In case of a PS PFS lamellae, the iron-rich PFS (Φ_{PFS} = 11%) forms spherical domains, which appeared as darkest domains due to the highest electron density (see Fig. 3 b). In case of PS cylinders, PFS domains could also be observed as spheres at the interface between the PS cylinders and the PMMA lamellae building an additional metallopolymer interlayer. Additionally, small-angle X-ray scattering (SAXS) measurements are performed to further investigate the triblock terpolymer morphology. The corresponding SAXS pattern of PS_{211}-*b*-PFS_{37}-*b*-$PMMA_{437}$ is given in Fig. 4 (blue).

In the SAXS patterns, the lamella structure seems to be dominant. For such a system the peak positions should obey the ratio 1:2:3 etc. As fitting model we used the sum of five Gaussian functions with fixed position ratios. Furthermore, a constant background and a term proportional to q^{-4} taking Porod-scattering into account was added. The resulting fit of the data is shown in Fig. 4 as solid black line, giving a very good description. From the position of the first peak a lamellar spacing of 33.5 ± 0.2 nm was found, which is in good agreement taking the lamellar morphology in Fig. 3 into account.

In case of PS_{250}-*b*-PFS_{39}-*b*-$P2VP_{551}$ having volume fractions of 29% for PS, 9% for PFS and 62% for P2VP, a cylindrical morphology for PS in a matrix of P2VP and a spherical sub-morphology of PFS at the cylinder-matrix interphase can be found as shown in Fig. 5. Interestingly, the dark domains in the middle of each PS cylinder domain can be assigned to the PFS domains due to the highest electron contrast for the metallopolymer, which might be obtained because of about 13% diblock copolymer impurities of PS_{250}-*b*-PFS_{32} precursor as already described in the section before (see also Fig. S4).

Additionally, scanning TEM (STEM) measurements operating in dark-field mode was used to further evidence the suggested morphology of P2VP-containing triblock terpolymer PS_{250}-*b*-PFS_{39}-*b*-$P2VP_{551}$. In contrast to TEM measurements in bright field mode, STEM images using a dark-field detector revealing an inverted black-white contrast. As given in Fig. 6 the cylindrical morphology was confirmed, however, the morphology at the interlayer surrounding the PS cylinders revealed no continuous domain for the metallopolymer PFS. Structures of cylinders in a matrix with spheres of the middle block segment at the interface were also described for example by Stadler and co-workers for a SBM BCP system [60]. Furthermore, the bright spherical or cylindrical PFS domains in the middle of each PS cylinder, which is probably caused by the presence of residual PS_{250}-*b*-PFS_{32} precursor are well

Table 2
Data for glass transition temperatures (T_g) and melting points (T_m) of synthesized tri- and pentablock terpolymers by DSC measurements applied with a heat rate of 10 K min^{-1} under nitrogen atmosphere.

Polymer	$T_{g\ PS/P2VP}$/°C	$T_{g\ PMMA}$/°C	$T_{m\ PFS}$/°C
PS_{211}-*b*-PFS_{37}-*b*-$PMMA_{437}$	101	≈128	≈133
PS_{250}-*b*-PFS_{39}-*b*-$P2VP_{551}$	99		129
PS_{230}-(*b*-PFS_{15}-*b*-$PMMA_{118}$)$_2$	101	≈128	≈132
PS_{231}-(*b*-PFS_{16}-*b*-$P2VP_{95}$)$_2$	97		132

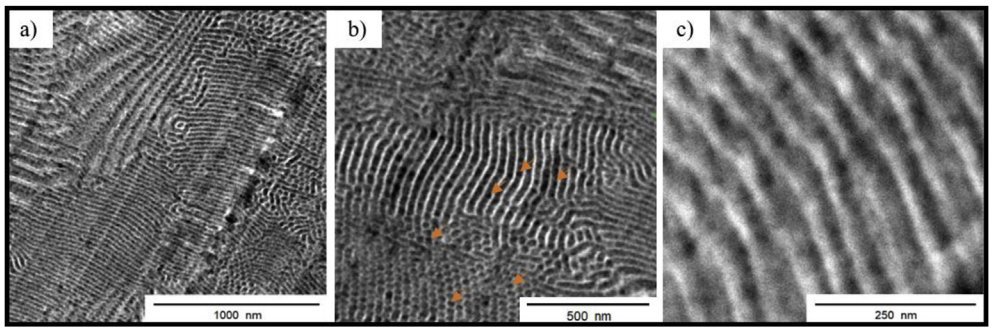

Fig. 3. TEM images of PS_{211}-*b*-PFS_{37}-*b*-$PMMA_{437}$ ultrathin slices without staining. Polymer bulk samples were prepared by slowly evaporating from methylene chloride followed by thermal annealing at 160 °C of the remaining films under nitrogen atmosphere for 36 h. Dark appearing domains correspond to the metallopolymer domains. Scale bars correspond to 1000 nm (a), 500 nm (b) and 250 nm (c).

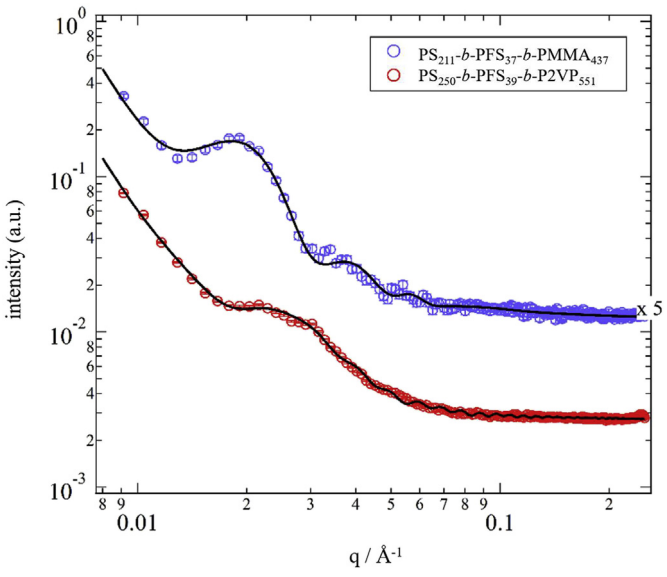

Fig. 4. SAXS patterns of PS_{211}-*b*-PFS_{37}-*b*-$PMMA_{437}$ (blue) and PS_{250}-*b*-PFS_{39}-*b*-$P2VP_{551}$ (red) the latter is shifted vertically for clarity. Solid lines depicted fits to a lamellar and cylindrical model respectively. See text for details. (For interpretation of the references to colour in this figure legend, the reader is referred to the Web version of this article.)

displayed featuring a diameter of 11 ± 2 nm and a cylinder distance of about 74 ± 4 nm. The diameter of the PS cylinders were found to be 39 ± 3 nm and the diameter of the PS cylinder surrounded by PFS spheres was determined to be 8 ± 2 nm.

The corresponding SAXS pattern of PS_{250}-*b*-PFS_{39}-*b*-$P2VP_{551}$ is additionally given in Fig. 4 (red) revealing a significantly different scattering pattern compared to PS_{211}-*b*-PFS_{37}-*b*-$PMMA_{437}$. Since clear scattering peaks were missing and only a broad shoulder was visible, precise fitting turned out to be difficult. Based on the TEM images, a model for hexagonal arranged cylinders was used for data description [61]. The scattering profile was described by the sum of Bragg peaks resulting from a hexagonal lattice of cylinders with cylinder distance and diameter being the important parameters. Starting from the parameters found by STEM a reasonable description of the scattering pattern was achieved. The distance between cylinder cores was found to be 60 nm, while the diameter of the cylinders was found to be 30 nm. As already mentioned for the PS_{250}-*b*-PFS_{39}-*b*-$P2VP_{551}$ morphology, the inner PFS domains in the middle of the PS cylinders is considered to be caused by residual PS_{250}-*b*-PFS_{32} precursor (amount was determined to be 13%). The amount of diblock copolymer significantly influenced the triblock copolymer morphology. Therefore, we additionally investigated the morphology of the original triblock copolymer blended with 38% diblock copolymer prior to inverse precipitation. Corresponding TEM images are displayed in Fig. S8 revealing a complex morphology of cylinders in a matrix for the PS_{250}-*b*-PFS_{32} ($\Phi_{PS/PFS}$ 80/20) on the one side and a mixed lamellar/cylinder morphology for PS_{250}-*b*-PFS_{39}-*b*-$P2VP_{551}$ influenced by the presence of PS_{250}-*b*-PFS_{32} on the other side. For the pure diblock copolymer morphology, the PFS cylinders revealed a diameter of 11 ± 2 nm, which is in good agreement with the PFS-containing domains in the middle of the PS cylinders of the purified PS_{250}-*b*-PFS_{39}-*b*-$P2VP_{551}$ (*cf.* Figs. 5 and 6). The distance between each cylinder was determined as 20 ± 2 nm. The lamellar morphology in Fig. S8 corresponds to the triblock terpolymer with bright P2VP lamellae and grey lamellae with darker spherical domains in the middle of the

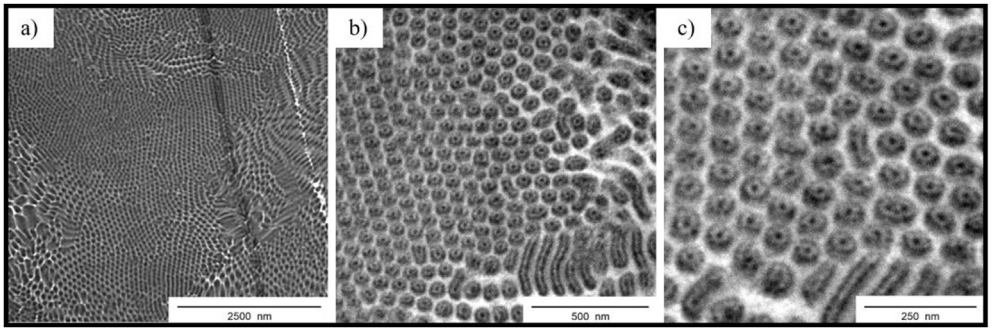

Fig. 5. TEM images of PS_{250}-*b*-PFS_{39}-*b*-$P2VP_{551}$ ultrathin slices without staining. Polymer bulk samples were prepared by slowly evaporating from methylene chloride followed by thermal annealing at 160 °C of the remaining films under nitrogen atmosphere for 36 h. Dark appearing domains correspond to the metallopolymer domains. Scale bars correspond to 2500 nm (a), 500 nm (b) and 250 nm (c).

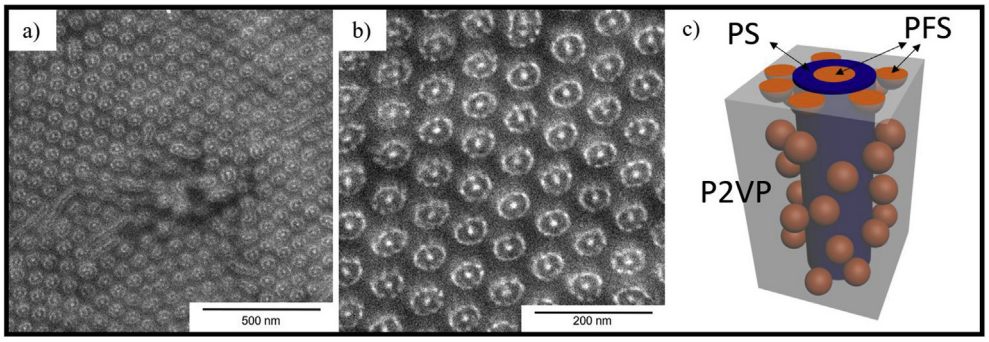

Fig. 6. STEM images of PS_{250}-*b*-PFS_{39}-*b*-$P2VP_{551}$ ultrathin slices without staining. Polymer bulk samples were prepared by slowly evaporating from methylene chloride followed by thermal annealing at 160 °C of the remaining films under nitrogen atmosphere for 36 h. Bright appearing domains correspond to the metallopolymer domains. Scale bars correspond to 500 nm (a) and 200 nm (b). Scheme of the corresponding morphology: cylinders of PS in a matrix of P2VP with PFS spheres at the surface of the PS cylinders. Additional PFS morphologies (orange) build the complex structure in the middle and at the surface of each PS cylinder (c). (For interpretation of the references to colour in this figure legend, the reader is referred to the Web version of this article.)

lamellae and at the surface, corresponds to PFS from the triblock terpolymer and diblock copolymer precursor. The lamellae distance between two bright lamellae was determined to be 60 ± 5 nm. Additional SAXS measurements were carried out for the blend system (Fig. S9). The observed pattern is a complex combination of scattering from both structures observed in the corresponding TEM image, *i.e.* lamellae and hexagonally arranged cylinders. According to results obtained from the TEM image, the first order peak of the lamellar structure is positioned around $q = 0.01$ Å^{-1} and thus indistinguishable from the primary beam. However, the second order peak slightly above $q = 0.02$ Å^{-1} allows for a good determination of the lamellar long spacing $d = 60$ nm, again, in good agreement with TEM results. The third order peak at $q = 0.03$ Å^{-1} featured a significantly increased intensity because it is enhanced by the first order peak of the hexagonal arranged cylinders. From the position of the peak a center-to-center distance of the cylinders of 23 nm is deduced, which is in accordance with TEM results. The solid black line in Fig. S9 is a guide for the eye showing the incoherent addition of scattering from lamellar and cylindrical regions, leading to a reasonable description of experimental data.

TEM images for the PMMA-containing pentablock terpolymer

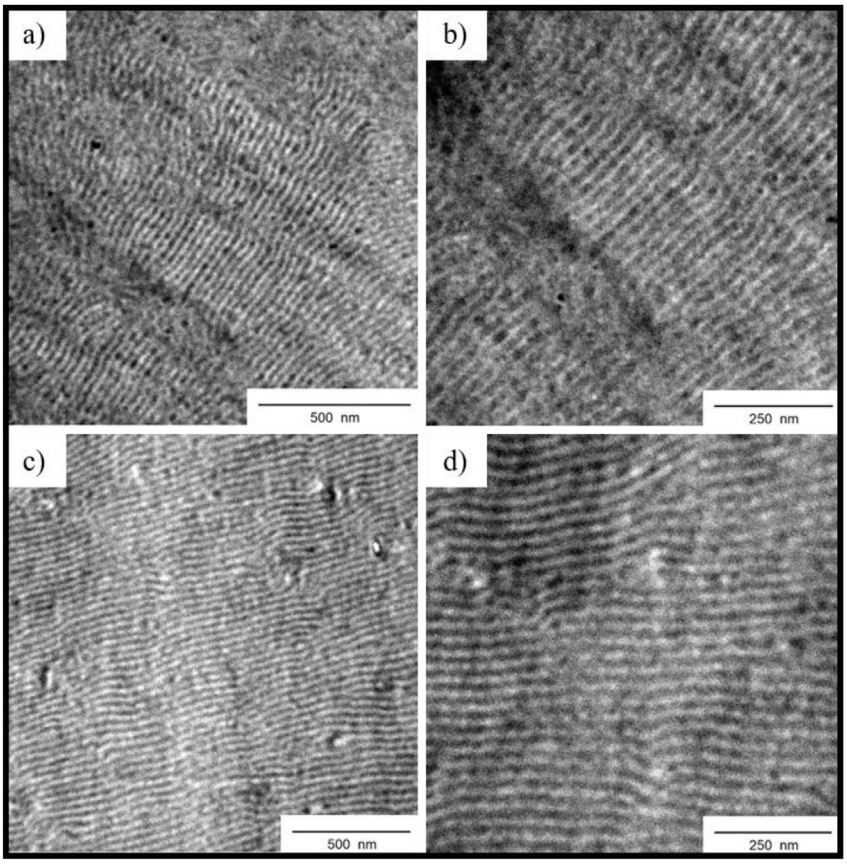

Fig. 7. TEM images of PS_{230}-(*b*-PFS_{15}-*b*-$PMMA_{118}$)$_2$ (a, b) and PS_{231}-(*b*-PFS_{16}-*b*-$P2VP_{95}$)$_2$ (c, d) after ultramicrotoming. Polymer bulk samples were prepared by slowly evaporating methylene chloride followed by thermal annealing at 160 °C of the remaining films under nitrogen atmosphere for 40 h. Dark appearing domains correspond to the metallopolymer-containing domains. Scale bars correspond to 500 nm (a, c) and 250 nm (b, d).

PS_{230}-(*b*-PFS_{15}-*b*-$PMMA_{118}$)$_2$ are given in Fig. 7 (a, b) revealing a lamellar morphology with a distance between two lamellae of about 28 ± 3 nm. The bright domains showed lamellae with a size of 10 ± 1 nm. Again, the dark appearing lamellae corresponded to the PFS segments having a volume fraction of 12%. It can be assumed that due to the short polymer length and the slight miscibility for PFS in the PS domains, with a volume content of 47%, gathered from the much higher incompatibility of PFS with PMMA than with PS [62]. Hence, the bright thin lamellae consist of PMMA having a volume fraction of 41%. A phase separation between the PS and PFS segments could not be clearly observed maybe due to the presence of only short PFS chains. Therefore, a partial miscibility of the block segments is possible. Additional SAXS measurements of PS_{230}-(*b*-PFS_{15}-*b*-$PMMA_{118}$)$_2$ were performed, as given in Fig. 8 (blue). A pronounced scattering peak around $q^* = 0.025$ Å^{-1} was clearly visible as well as a much weaker second order peak at $2q^*$. A fit of several Guassian functions as described above yielded a good description of the scattering data. The distance between two lamellae was found to be 23.8 ± 0.1 nm in accordance with the results derived by TEM investigations.

In case of the P2VP-containing pentablock terpolymer PS_{231}-(*b*-PFS_{16}-*b*-$P2VP_{95}$)$_2$ a similar lamellar morphology was found as given in the TEM images in Fig. 7(c and d). The distance between both lamellae was determined to be 29 ± 3 nm, while each dark lamella featured a size of about 16 ± 2 nm. Taking the thickness of each lamella and the different volume fractions into account, it can be assumed that PS (49%) formed the bright and PFS (13%) together with P2VP (38%) the dark domain. As already mentioned for the PMMA containing pentablock terpolymer, a phase separation of PFS in the dark appearing domain could not be observed, which might be due to the only short PFS chains, *i.e.* only 16 repeating units of FS monomer within the PFS block segment, or limited resolution of the TEM. The lamellar morphology is also confirmed by SAXS measurements. In Fig. 8 (red) the scattering data and the according model description is depicted. From the position of the lamellar peak sequence a distance between two lamellae of (30.2 ± 0.1) nm was obtained, which is in very good agreement with results found via TEM.

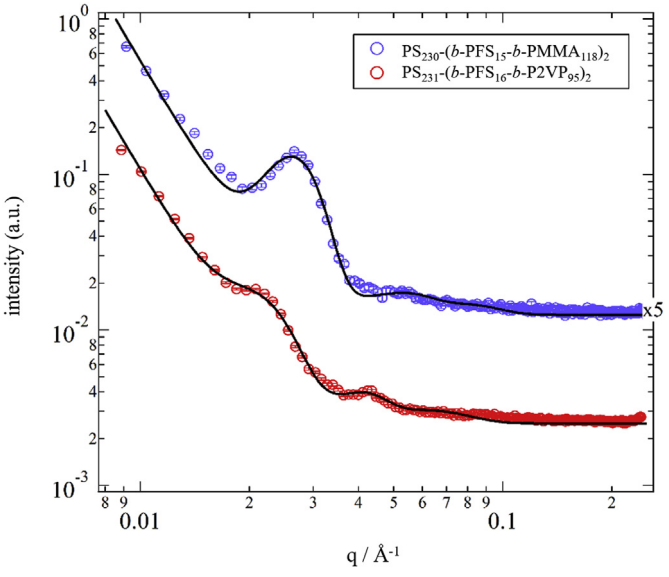

Fig. 8. SAXS patterns of PS_{230}-(*b*-PFS_{15}-*b*-$PMMA_{118}$)$_2$ (blue) and PS_{231}-(*b*-PFS_{16}-*b*-$P2VP_{95}$)$_2$ (red) the latter is shifted vertically for clarity. Solid lines depicted fits from a lamellar model. See text for details. (For interpretation of the references to colour in this figure legend, the reader is referred to the Web version of this article.)

4. Conclusion

In conclusion, the preparation of ABC and CBABC tri- and pentablock terpolymers bearing polystyrene (PS), poly(1,1′-dimethylsilaferrocenophane) (PFS) and poly(methyl methacrylate) (PMMA) or poly(2-vinylpyridine) (P2VP) segments by sequential anionic polymerization was reported. Molar masses up to 90 kg mol^{-1} and well-defined – with respect to composition and constitution – polymers with low dispersity index values, *Đ*, were obtained as evidenced by SEC, NMR spectroscopy and DSC measurements. Furthermore, microphase separation for all metal-containing polymers having a comparably short PFS segment was proven by TEM, STEM and SAXS measurements. For the triblock terpolymers lamellar or cylindrical morphologies were found having PS cylinders in a P2VP matrix, while the cylinders featured a PFS-containing core morphology surrounded by an additional spherical morphology of PFS domains. Domain sizes and type of morphologies were corroborated by SAXS measurements. Finally, the PFS-containing symmetrical CBABC pentablock terpolymers revealed clear lamellar structures. We expect that the results from the present study of the structure formation of tri- and pentablock terpolymers pave the way for applications in the nanolithography sector or moreover as stimuli-responsive materials like the change of the wetting-behavior due to the present of corresponding moieties, which will also be part of further investigations.

Acknowledgements

The authors acknowledge partial support in the frame of the LOEWE project iNAPO by the Hessen State Ministry of Higher Education, Research and the Arts. Additionally, the authors thank Prof. Dr. H.-J. Kleebe and Dr. Lauterbach (Institute of Applied Geosciences, TU Darmstadt) for their support with (S)TEM measurements. The authors also thank Annika Schlander for artwork support.

Appendix A. Supplementary data

Supplementary data to this article can be found online at https://doi.org/10.1016/j.jorganchem.2019.01.001.

References

[1] C.M. Bates, F.S. Bates, Macromolecules 50 (2017) 3–22.
[2] Y. Mai, A. Eisenberg, Chem. Soc. Rev. 41 (18) (2012) 5969–5985.
[3] M. Stefik, S. Guldin, S. Vignolini, U. Wiesner, U. Steiner, Chem. Soc. Rev. 44 (15) (2015) 5076–5091.
[4] M. Lazzari, G. Liu, S. Lecommandoux, Block Copolymers in Nanoscience, Wiley-VCH, Weinheim, 2006.
[5] T. Smart, H. Lomas, M. Massignani, M.V. Flores-Merino, L.R. Perez, G. Battaglia, Nano Today 3 (3–4) (2008) 38–46.
[6] A. Checco, A. Rahman, C.T. Black, Adv. Mater. 26 (6) (2014) 886–891.
[7] S. Park, X. Cheng, A. Boker, L. Tsarkova, Adv. Mater. 28 (32) (2016) 6900–6905.
[8] S. Schöttner, H.-J. Schaffrath, M. Gallei, Macromolecules 49 (19) (2016) 7286–7295.
[9] S.P. Nunes, Macromolecules 49 (8) (2016) 2905–2916.
[10] M.A.C. Stuart, W.T.S. Huck, J. Genzer, M. Müller, C. Ober, M. Stamm, G.B. Sukhorukov, I. Szleifer, V.V. Tsukruk, M. Urban, F. Winnik, S. Zauscher, I. Luzinov, S. Minko, Nature (2010) 101–113.
[11] J.K. Kim, S.Y. Yang, Y. Lee, Y. Kim, Prog. Polym. Sci. 35 (2010) 1325–1349.
[12] F.H. Schacher, P.A. Rupar, I. Manners, Angew. Chem. Int. Ed. 51 (32) (2012) 7898–7921.
[13] J. Zhou, G.R. Whittell, I. Manners, Macromolecules 47 (2014) 3529–3543.
[14] B.V.K.J. Schmidt, J. Elbert, C. Barner-Kowollik, M. Gallei, Macromol. Rapid Commun. 35 (2014) 708–714.
[15] R.H. Staff, M. Gallei, K. Landfester, D. Crespy, Macromolecules 47 (2014) 4876–4883.
[16] F.A. Plamper, Adv. Polym. Sci. 266 (2014) 125–212.
[17] C. Rüttiger, V. Pfeifer, V. Rittscher, D. Stock, D. Scheid, S. Vowinkel, F. Roth, H. Didzoleit, B. Stühn, J. Elbert, E. Ionescu, M. Gallei, Polym. Chem. 7 (2016) 1129–1137.

[18] M. Appold, C. Mari, C. Lederle, J. Elbert, C. Schmidt, I. Ott, B. Stühn, G. Gasser, M. Gallei, Polym. Chem. 8 (2017) 890–900.
[19] R. Glass, M. Möller, J.P. Spatz, Nanotechn. 14 (2003) 1153–1160.
[20] C.G. Hardy, L. Ren, J. Zhang, C. Tang, Isr. J. Chem. 52 (2012) 230–245.
[21] Y. Yan, J. Zhang, L. Ren, C. Tang, Chem. Soc. Rev. 45 (19) (2016) 5232–5263.
[22] C.G. Hardy, J. Zhang, Y. Yan, L. Ren, C. Tang, Prog. Polym. Sci. 39 (2014) 1742–1796.
[23] R. Pietschnig, Chem. Soc. Rev. 45 (2016) 5216–5231.
[24] M. Gallei, Macromol. Chem. Phys. 215 (2014) 699–704.
[25] M. Gallei, C. Rüttiger, Chem. Eur J. 24 (2018) 10006–10021.
[26] I. Manners, Can. J. Chem. 76 (1998) 371–381.
[27] V. Bellas, M. Rehahn, Angew. Chem. Int. Ed. 46 (2007) 5082–5104.
[28] A.D. Russell, R.A. Musgrave, L.K. Stoll, P. Choi, H. Qiu, I. Manners, J. Organomet. Chem. 784 (2015) 24–30.
[29] D.A. Foucher, B.-Z. Tang, I. Manners, J. Am. Chem. Soc. 114 (1992) 6246–6248.
[30] F.S. Bates, G.H. Fredrickson, Phys. Today 52 (2) (1999) 32.
[31] N. Hadjichristidis, H. Iatrou, M. Pitsikalis, S. Pispas, A. Avgeropoulos, Prog. Polym. Sci. 30 (7) (2005) 725–782.
[32] H.-H. Liu, C.-I. Huang, A.-C. Shi, Macromolecules 48 (17) (2015) 6214–6223.
[33] H. Jinnai, T. Kaneko, K. Matsunaga, C. Abetz, V. Abetz, Soft Matter 5 (10) (2009) 2042.
[34] Y. Tanaka, H. Hasegawa, T. Hashimoto, A. Ribbe, K. Sugiyama, A. Hirao, S. Nakahama, Polym. J. 31 (1999) 989–994.
[35] H. Elbs, K. Fukunaga, R. Stadler, G. Sauer, R. Magerle, G. Krausch, Macromolecules 32 (1999) 1204–1211.
[36] T. Goldacker, V. Abetz, R. Stadler, I. Erukhimovich, L. Leibler, Nature 398 (1999) 137–139.
[37] H. Hückstädt, A. Göpfert, V. Abetz, Polymer 41 (2000) 9089–9094.
[38] A.J. Meuler, G. Fleury, M.A. Hillmyer, F.S. Bates, Macromolecules 41 (2008) 5809–5817.
[39] E. Dashtimoghadam, H. Salimi-Kenari, V. Forooqi Motlaq, M.M. Hasani-Sadrabadi, H. Mirzadeh, K. Zhu, K.D. Knudsen, B. Nyström, Eur. Polym. J. 97 (2017) 158–168.
[40] C. Tsitsilianis, N. Stavrouli, V. Bocharova, S. Angelopoulos, A. Kiriy, I. Katsampas, M. Stamm, Polymer 49 (13–14) (2008) 2996–3006.
[41] R.F. Storey, A.D. Scheuer, B.C. Achord, Polymer 46 (7) (2005) 2141–2152.
[42] S. Behzadi, M. Gallei, J. Elbert, M. Appold, G. Glasser, K. Landfester, D. Crespy, Polym. Chem. 7 (20) (2016) 3434–3443.
[43] D.A. Rider, I. Manners, Polym. Rev. 47 (2) (2007) 165–195.
[44] H.K. Choi, J. Gwyther, I. Manners, C.A. Ross, ACS Nano 6 (2012) 8342–8348.
[45] H.K. Choi, N.M. Aimon, D.H. Kim, X.Y. Sun, J. Gwyther, I. Manners, C.A. Ross, ACS Nano 8 (2014) 9248–9254.
[46] A. Nunns, C.A. Ross, I. Manners, Macromolecules 46 (7) (2013) 2628–2635.
[47] C. Kloninger, M. Rehahn, Macromol. Chem. Phys. 208 (8) (2007) 833–840.
[48] V.P. Chuang, C.A. Ross, J. Gwyther, I. Manners, Adv. Mater. 21 (37) (2009) 3789–3793.
[49] U. Datta, M. Rehahn, Macromol. Rapid Commun. 25 (18) (2004) 1615–1622.
[50] C. Kloninger, M. Rehahn, Macromolecules 37 (2004) 1720–1727.
[51] L. Vanderark, E. Januszewski, J. Gwyther, I. Manners, Eur. Polym. J. 47 (4) (2011) 823–826.
[52] C. Kloninger, M. Rehahn, Macromolecules 37 (2004) 1720–1727.
[53] C. Rüttiger, H. Hübner, S. Schöttner, T. Winter, B. Kuttich, B. Stühn, M. Gallei, ACS Appl. Mater. Interfaces 10 (4) (2018) 4018–4030.
[54] M. Gallei, R. Klein, M. Rehahn, Macromolecules 43 (2010) 1844–1854.
[55] M. Kraska, M. Gallei, B. Stühn, M. Rehahn, Langmuir 29 (2013) 8284–8291.
[56] J.I. Brandrup, E.A. Edmund, H. Grulke, A. Abe, D.R. Bloch, Polymer Handbook, John Wiley&Sons, 1999.
[57] R.G.H. Lammertink, M.A. Hempenius, E.L. Thomas, G.J. Vancso, J. Polym. Sci., Part B: Polym. Phys. 37 (1999) 1009–1021.
[58] S.K. Varshney, C. Jacobs, J.-P. Hautekeer, P. Bayard, R. Jéróme, R. Fayt, P. Teyssié, Macromolecules 24 (1991) 4997–5000.
[59] A.P. Soto, I. Manners, Macromolecules 42 (2009) 40–42.
[60] U. Breiner, U. Krappe, V. Abetz, R. Stadler, Macromol. Chem. Phys. 198 (1997) 1051–1083.
[61] M. Schwab, B. Stühn, Colloid Polym. Sci. 275 (1997) 341–351.
[62] C. Kloninger, Synthese und morphologische Charakterisierung von Blockcopolymeren aus Metallorganischen und Organischen Segmenten, Macromolecular Chemistry Department, Technische Universität Darmstadt, Darmstadt, Germany, 2004, p. 198.